Yeung, Dennis; Farina, Dario; Vujaklija, Ivan

Can Multi-DoF Training Improve Robustness of Muscle Synergy Inspired Myocontrollers?

Published in:
Proceedings of the 16th IEEE International Conference on Rehabilitation Robotics, ICORR 2019

DOI:
10.1109/ICORR.2019.8779520

Published: 01/06/2019

Document Version
Peer reviewed version

Please cite the original version:
Yeung, D., Farina, D., & Vujaklija, I. (2019). Can Multi-DoF Training Improve Robustness of Muscle Synergy Inspired Myocontrollers? In *Proceedings of the 16th IEEE International Conference on Rehabilitation Robotics, ICORR 2019* (Vol. 2019, pp. 665-670). (IEEE International Conference on Rehabilitation Robotics). IEEE. https://doi.org/10.1109/ICORR.2019.8779520

Can Multi-DoF Training Improve Robustness of Muscle Synergy Inspired Myocontrollers?*

Dennis Yeung, Dario Farina, *Fellow, IEEE*, and Ivan Vujaklija, *Member, IEEE*

***Abstract*— Non-negative Matrix Factorization (NMF) has been effective in extracting commands from surface electromyography (EMG) for the control of upper-limb prostheses. This approach enables Simultaneous and Proportional Control (SPC) over multiple degrees-of-freedom (DoFs) in a minimally supervised way. Here, like with other myoelectric approaches, robustness remains essential for clinical adoption, with device donning/doffing being a known cause for performance degradation. Previous research has demonstrated that NMF-based myocontrollers, trained on just single-DoF activations, permit a certain degree of user adaptation to a range of disturbances. In this study, we compare this traditional NMF controller with its sparsity constrained variation that allows initialization using both single and combined-DoF activations (NMF-C). The evaluation was done on 12 able bodied participants through a set of online target-reaching tests. Subjects were fitted with an 8-channel bipolar EMG setup, which was shifted by 1cm in both transversal directions throughout the experiments without system retraining. In the baseline condition NMF performed somewhat better than NMF-C, but it did suffer more following the electrode repositioning, making the two perform on par. With no significant difference present across the conditions, results suggest that there is no immediate advantage from the naïve inclusion of more comprehensive training sets to the classic synergy-inspired implementation of SPC.**

I. Introduction

Surface electromyography (sEMG) constitutes one of the most common non-invasive interfaces between upper-limb amputees and powered prostheses [1]. However, commercially available devices almost solely rely on basic, sequential control methods that tend to be perceived as highly unintuitive and limited in function [2]. This lack of satisfactory interface has further contributed to the current high rate of prosthetic abandonment [3], [4].

The inadequacies of existing clinical solutions have therefore spurred research efforts into more advanced control approaches. The most prominent of recent approaches involve pattern recognition based intention classification [5], [6], regression based motion estimation [7]–[9], and musculoskeletal modeling of the missing limb [10], [11]. Each of these approaches comes with its own pros and cons however, the increased functionality is commonly followed by the decreased robustness as controller performance becomes sensitive to non-stationarities caused by environmental factors, such as perspiration, muscle fatigue and electrode displacement [12]–[14].

The intuitive mapping established by regression based systems has been shown to allow users to adapt to the control scenarios, to a certain degree, even in case of sudden noise onsets [15] or electrode repositioning [16]. These algorithms tend to provide users with a possibility to compensate for the introduced instability and restore some functionality by this adaptation. Co-adaptive learning approach using recursive least squares [17] has been demonstrated as an effective way of further dealing with non-stationarities in regression based controllers. However, this is essentially a supervised approach which requires exact target labels in order for it to adapt, making it less applicable in real-life conditions. Moreover, it is highly dependent on the selected parameter values, which, if not fully optimized, can lead to further instabilities and performance deterioration.

To deal with perturbations, pattern recognition based controllers have resorted to extending the training data sets as to include more descriptive and generalized data [13], [18]. This has been shown as a promising approach, however it may determine over-fitting.

In this study, we are aiming to investigate whether a similar approach of training on a diverse dataset will lead to an increase in robustness of the muscle synergy inspired regression based myocontrollers. Muceli et al. [16] have previously shown that this type of controller, trained strictly on single Degree of Freedom (DoF) motions, allows users to adapt and restore a certain degree of functionality following electrode repositioning. Lin et al. [19] have proposed a sparseness constraint extension of the same controller which allowed multi-DoF training data to be used. Here, we compare the two approaches and investigate how robust they are against medial and transversal electrode shifts using a set of real-time virtual reality (VR) tasks.

II. Methods

A. Controller Design

Non-negative Matrix Factorization (NMF) has been previously used [7], [20] for establishing regression based controllers. By adopting dimensionality reduction based on the assumption that multiple muscles act concurrently (synergistically) in order to execute an intended motion, NMF allows synergy matrix estimation from observed EMG signals. We adopt the model proposed by Jiang et al. [20]:

$$\hat{\mathrm{X}} = \mathrm{WF} \tag{1}$$

* Research supported by the European Union's Horizon 2020 research and innovation program under grant agreement number 687795 (project INPUT).

D.Y and I.V. are with the Department of Electrical Engineering and Automation, Aalto University, Espoo, Finland (correspondence to: e-mail: ivan.vujaklija@aalto.fi, +358504707760; dennis.yeung@aalto.fi).

D. F. is with the Department of Bioengineering, Imperial College London, London, UK (e-mail: d.farina@imperial.ac.uk).

where $\hat{X}$ is the $N \times M$ observation matrix, with N denoting the number of EMG channels and M the number of samples (root mean square (RMS) values) per channel. W represents a $N \times D$ synergy matrix estimation over D DoFs. F is a $D \times M$ matrix of latent control signals describing the intended motions.

In order to obtain the synergy matrix W, the NMF is based on a multiplicative update rule [21] according to which the squared Euclidian error cost-function given by (2) is minimized using the update rules (3) and (4):

$$\varepsilon = \frac{1}{2}\left\|\hat{X} - WF\right\|^2 = \frac{1}{2}\sum_{i=1}^{N}\sum_{j=1}^{M}(\hat{X}_{ij} - (WF)_{ij})^2 \quad (2)$$

$$F_{dj} \leftarrow F_{dj}\frac{(W^T X)_{dj}}{(W^T WF)_{dj}} \quad (3)$$

$$W_{id} \leftarrow W_{id}\frac{(XF^T)_{id}}{(WFF^T)_{id}} \quad (4)$$

where $d \in [1,..,2D]$.

Estimation of the command signals (F) in real-time ($\hat{f}(t)$) can then be done by multiplying the pseudo-inverse of the synergy matrix (W^+) with the incoming EMG feature vector ($x(t)$) as follows:

$$\hat{f}(t) = W^+ x(t) \quad (5)$$

where $\hat{f}(t) = [f_1^+, f_1^-, f_2^+, f_2^-, \ldots, f_D^+, f_D^-]^T$, with f_i^+ and f_i^- representing a positive and negative direction of the i-th DoF respectively (e.g. wrist rotation consists of pronation and supination).

The synergy matrix can be estimated from a training set including single DoF activations and then used to estimate multi-DoF commands concurrently based on Eq. (5). An effective way to include multi-DoF motions into the training data set (combined-DoF regressor training), Lin et al. [19] have proposed the introduction of a sparseness constraint on the command signals. Here, as described in [22], we induce sparseness by imposing the $L_{1/2}$ regularization on (2):

$$\varepsilon = \frac{1}{2}\left\|\hat{X} - WF\right\|^2 + \beta\|F\|_{1/2} = \frac{1}{2}\sum_{i=1}^{N}\sum_{j=1}^{M}(\hat{X}_{ij} - (WF)_{ij})^2 + \beta\sum_{j=1}^{N}\sqrt{F_{:,j}} \quad (6)$$

$$F_{dj} \leftarrow F_{dj}\frac{(W^T X)_{dj}}{\left(W^T WF + \frac{\beta}{2}F^{-\frac{1}{2}}\right)_{dj}} \quad (7)$$

with parameter β determining the trade-off between the reconstruction error and the amount of sparseness.

B. Subjects

Twelve subjects (1 left-handed female and 11 right-handed males, age: 22-31) volunteered to participate in the experiment. None of them had any known neurological disorder or had previously been extensively exposed to similar control paradigms. The local ethical committee of the Imperial College London (ICREC #18IC4685) approved the study and all the participants read and signed the informed consent.

C. Data Acquisition

Subjects seated comfortably in a chair in front of a computer screen with their arms relaxed by their side. Myo Armband, an 8 channel surface EMG acquisition wearable device (Thalamic Labs, Canada), was fitted on their dominant forearm. Placement was done so that channel 4 of the system (marked as the reference pod) lays flat on the muscle bulk located 2 cm below the lateral epicondyle. The positioning of the reference pod was then marked using a skin marker to ensure a precise landmark throughout the experiment. The data were sampled at 200 Hz and transferred via Bluetooth to the host computer for further processing.

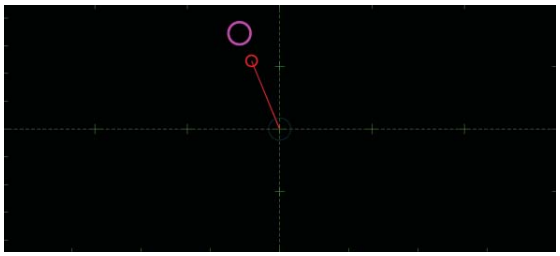

Figure 1. The virtual reaching task presented to subjects during online testing. In each session, subjects are asked to maneuver the red cursor as quickly as possible into a set of sequentially presented targets (magenta circles) within a time interval of 10 s.

D. Calibration Phase

The calibration of the controller was done using solely EMG signals acquired during free, dynamic movements. No additional kinematic or kinetic data was recorded for labeling. During the calibration, subjects were prompted by visual cues to first perform three repetitions of movements involving only one DoF at a time and then to perform three additional sets of concurrent activations. The focus of this study was on wrist flexion/extension (DoF1), and ulnar and radial deviation (DoF2). The data acquisition and visual guidance was provided using a custom Matlab® program.

Figure 2. Myo Armband placement on the right forearm of a subject. The transversal shifts of 1cm along the indicated directions have been induced in order to simulate prosthetic donning and doffing.

E. Parameter Search

To choose a suitable trade-off between the reconstruction error and the amount of sparseness, β, parameter search with 3-fold cross-validation was conducted on the calibration data acquired from a pilot test. Each subset of the training data (DoF1 trials, DoF2 trials, and combination trials) was partitioned across 3 folds. Within each fold, 2/3 of the data was used as the training set for model initialization with the particular β and the remaining 1/3 was used as the validation set. For each fold, the signal-to-noise ratio (SNR) was calculated as the ratio between total intended DoF activation

and total unintended DoF activation estimated from the single DoF trials of the validation set:

$$SNR = \frac{\sum_{t=1} \hat{f}_{int}(t)}{\sum_{t=1}^{T} \hat{f}_{unint}(t)} \quad (8)$$

where $\hat{f}_{int}(t)$ is the activation amplitude of the intended DoF at time t while $\hat{f}_{unint}(t)$ is the activation amplitude of the unintended DoF. Here, the intended DoF corresponds to the single DoF direction indicated by the visual cue at time t during the calibration phase. The SNR from each fold was then averaged. Values of β ranging from 1 to 50 were searched with best value yielding the lowest average SNR. While this chosen value would not be optimal for each individual subject, inclusion of the regularization term generally improves the SNR of factorized control signals as demonstrated in Fig. 3.

F. Online Testing

During the online testing phase, subjects were given the control of an on-screen cursor within the task space (Fig. 1). The planar displacements (horizontal and vertical) of the cursor were proportional to the estimated wrist movements - flexion/extension movements were mapped along the horizontal axis and ulnar/radial deviations represented the vertical shifts.

The online evaluation comprised six sessions. The first two sessions allowed subjects to operate either the single-DoF (NMF) or the combined-DoF (NMF-C) trained estimator with the initially trained electrode positions ("Unshifted"). In the remaining four sessions, the subjects did the same but following the transversal repositioning of the electrodes (Fig. 2). By rotating the electrode armband clock-wise around the right forearm, a 1-cm lateral shift was induced ("Lateral Shifted"). Correspondingly, the rotation in the opposite direction from the neutral position brought the reference sensor 1-cm closer to the medial epicondyle, resulting in the medial shift ("Medial Shifted").

Each session contained 24 virtual target-reaching tasks, which required subjects to steer the cursor inside the target circle with radii of 8 density-independent pixels (dp) in a 400x180dp task space (Fig. 1). The targets were equally spaced along two concentric rings. Eight targets were evenly distributed along the inner ring, 40dp from the origin, while 16 targets were positioned equidistant from one another along the outer ring, 75dp from the origin. In this way, subjects had to face a mixture of tasks requiring both single and simultaneous DoF control. For a target to be successfully reached, the cursor had to be kept inside the target circle for 0.5s and this had to be accomplished within the time limit of 10s. When a target was reached or when the time limit was exceeded, subjects were required to relax and return the cursor to the origin before the next task was presented. For each session, the order of the targets was randomized.

G.Performance Metrics

To evaluate the online performance of the two estimators, a set of previously introduced metrics [23] was computed. The Completion Rate (CR) of each trial indicated the ratio between the number of successfully completed tasks and their total number. Completion Time (CT) recorded the time required to reach the completed target and Path Efficiency (PE) indicated the ratio between the optimal path from the origin (straight line to the target) and the actual trajectory of the cursor. Throughput (TP) was used to measure the information transfer capabilities of the established interface and it represented the ratio of the given task's index of difficulty (ID) and the actual completion time:

$$TP = \frac{ID}{CT} \quad (9)$$

This measure is based on Shannon's Extension of Fitts' Law [24], [25], and in this case ID was expressed as a relationship between target displacement along the DoFs (D_1, D_2) and the target radius (r):

$$ID = \log_2 \left(\frac{\left(\frac{1}{2}D_1 + \frac{1}{2}D_2\right)^2}{r} + 1 \right) \quad (10)$$

H.Statistical Analysis

To test for statistical differences in the performance of the two estimators, a two-way repeated measures ANOVA (RM-ANOVA) was conducted with algorithm and electrode shift condition as factors. If a significant interaction was detected, multiple focused one-way RM-ANOVA was done, with one level fixed in each analysis where detected significance was followed by pairwise comparisons. If no significant interaction between the factors was detected, only the main effects were analyzed. The analysis was carried out using SPSS with significance level set as 0.05 for all tests. Mauchly's sphericity test was conducted prior to each analysis. If any significant difference between the variances was detected, Greenhouse-Geiser correction was applied.

III. Results

The experimental results are shown in Fig. 4. From the two-way RM-ANOVA's, significant interaction between controller and electrode shift was detected for CR ($F(2,22)=3.870$, $p=0.036$). For NMF, there was statistically significant difference in CR between electrode shift positions ($F(2,22)=8.906$, $p=0.001$) and the post-hoc analysis with Bonferonni adjustment revealed that Unshifted electrode positions had higher CR than Lateral Shifted with a mean difference of 0.20±0.05, $p=0.004$. This shows that, while using NMF, there was a significantly lower number of targets reached following the electrode repositioning. While there was a decrease in CR of NMF-C once the sensors have been relocated, the observed difference was not significant. However, its initial, Unshifted, CR performance was indeed lower to begin with in comparison to that of unperturbed NMF. At the same time, both controllers have achieved similar CRs following the electrode shifts.

The two-way RM-ANOVA applied on PE revealed no significant interaction between algorithm and electrode shift. However, the main effect of electrode shift showed statistically significant differences between sessions $F(2,22)=6.297$, $p=0.007$. PE was significantly higher in sessions with Unshifted electrodes compared to Lateral Shifted electrodes (5.408±1.517%, $p=0.013$) and Medial Shifted electrode positions (3.616±1.145, $p=0.027$).

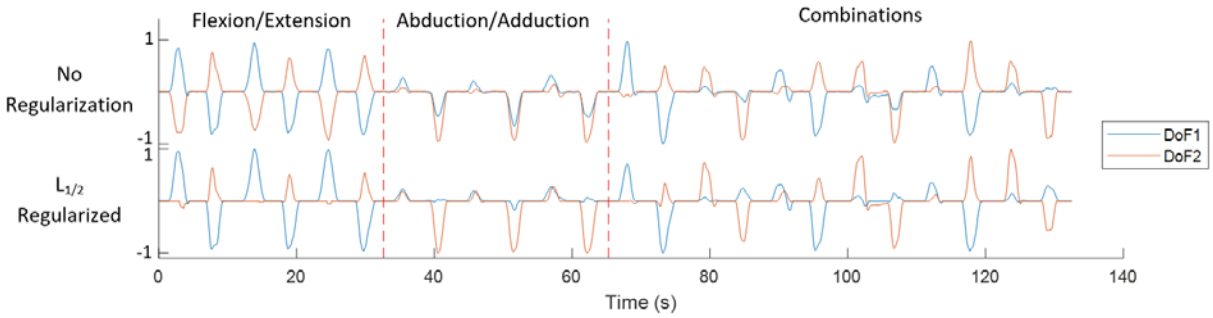

Figure 3. Latent command signals factorized from training data consisting of single and combined DoF wrist motions. By including $L_{1/2}$ regularization, sparsity is encouraged and unintended DoF activations become suppressed. Without this sparsity constraint, the relation between specific command signals and DoF directions become less clear. In both cases however, one basis was identified from the EMG patterns of combined adduction and flexion which are more localized. This command primitive has been assigned to the activation of DoF 2 in the positive direction. This is shown by the third activation in each set of four in the "Combinations" section of the figure.

Essentially, this shows that regardless of the used algorithm the PE became worse once the electrodes have been repositioned.

For CT, no significant interaction between the factors were found though significant differences were observed from the main effect of electrode shift ($F(2,22)=4.224$, $p=0.027$). CT's in sessions with Unshifted electrodes were significantly lower than those with Medial Shifted electrodes with a mean difference of 0.502 ± 0.159s, $p=0.028$. These results align with those of PE, indicating that both algorithms performed similarly and required longer times to reach the targets in the perturbed state.

Finally, no significant interaction or main effect was detected for TP.

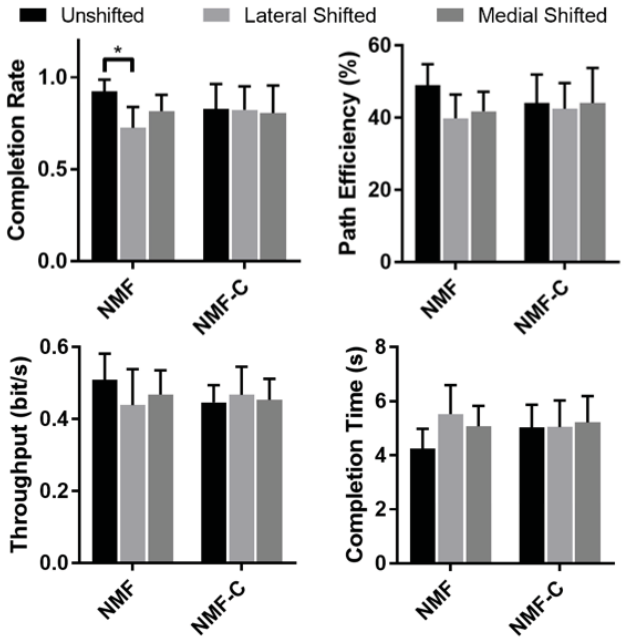

Figure 4. Performance metrics across all six sessions where * indicates statistical significance of simple main effects. The Completion Rate of NMF control was found to be significantly lower in Lateral Shifted electrode conditions compared to Unshifted. With both algorithms pooled, Path Efficiency was found to be significantly lower in Lateral and Medial Shifted sessions compared to Unshifted. Similarly, ignoring the effects of algorithm, Completion Time was found to be significantly higher in Medial Shifted sessions compared to Unshifted.

IV. Discussions

The effect of electrode shift was tested for two conceptually similar myoelectric controllers based on the minimally supervised extraction of muscle synergies. The first type (NMF) was trained using only the essential dataset containing single-DOF activations known to deliver a highly intuitive mapping. While initial performance was high under normative conditions, deterioration in control was noticeable after introduction of 1-cm transversal shifts to the electrode array. The second controller (NMF-C) was trained on both single and combined DoF activations. This produced a controller that was less intuitive to use and yielded inferior performance as compared to NMF under ideal conditions. However, following the electrode shifts, NMF-C seem to have not lost much of its initial controllability and thus, in relative terms, has been less affected by the perturbations. Nevertheless, the general performance of both controllers in the perturbed states was comparable.

With NMF, muscle activations of orthogonal wrist movements, flexion/extension and abduction/adduction, were respectively mapped to the horizontal and vertical displacement of the cursor. In the unperturbed state, this controller allowed subjects to perform target reaching tasks with high precision and efficiency. Furthermore, despite only being trained on single-DoF activations, the resultant mapping also provided intuitive control for combined-DoF actions, a characteristic that is consistent with past studies [7], [16]. However, when the electrode shifts were introduced, subjects were unable to navigate the full task space as natural muscle activations were interpreted as conflicting within-DoFs commands, as shown in an exemplary case in Fig. 5. This can be attributed to the higher density of synergy matrices, a by-product of the traditional "divide and conquer" initialization (Fig. 6). While the method addresses the indeterminacy of NMF by restricting the possible solution space and extracting antagonistic synergies for each DoF separately, it also results in sensitivities for opposing directions being proximal to one another such that electrode shifts would increase the amount of within-DoF co-activations.

With NMF-C, all synergies are concurrently extracted from the entire repertoire of training activations, resulting in somewhat sparser weight matrices, as shown in Fig. 6. This makes the controller less affected by the electrode shift as individual DoF activations are more separated in sensor space.

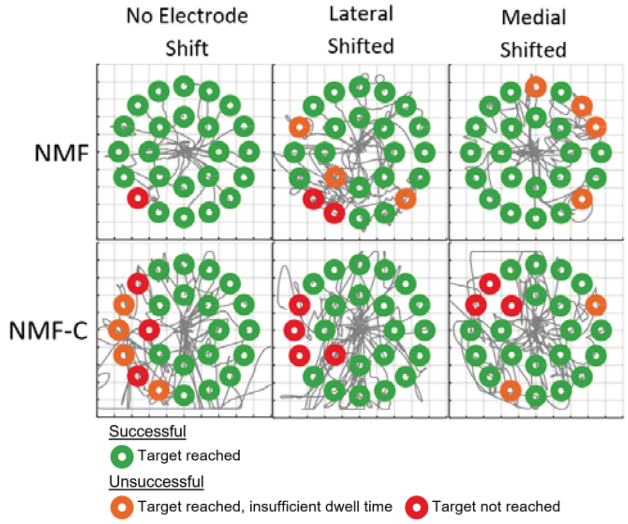

Figure 5. Session trajectories from Subject 7 with colored circles representing the targets. When electrodes were shifted, access to the full solution-space was restricted with the DoF-wise trained NMF controller. In contrast, control with the multi-DoF trained NMF-C controller did not deteriorate with electrode shift with both controllers achieving similar target hit rates during the perturbed scenarios.

By minimizing the within-DoF command conflicts that restrict the full exploration of the task space, target reaching capabilities are preserved between sessions despite the introduced perturbations. It should be highlighted that for this particular set of wrist movements, combined DoF motions can produce EMG patterns that are more localized compared to single DoF motions. While there is overlap in the recruitment of muscles for flexion/extension and abduction/adduction, combined motions tend to rely more on the subset of muscles that are activated during each individual DoF movement. With regards to the extraction of additive basis features, the factorization algorithm then naturally favors assigning EMG patterns associated with combined DoF motions as the building blocks in the decomposition. This can be seen in Fig. 3 where single DoF command signals were activated during combined DoF wrist movements and vice-versa. Indeed, assigning the extracted synergies to vertical and horizontal excitations in the task space can become ambiguous unless sparsity constraints are applied to the command primitives. Nonetheless, even the constrained solution results in mappings that are rotationally distorted, with subjects reporting irregular sensitivities between the different sectors of the task space.

Muceli et al. [16] conducted a similar study of electrode shift effects on DoF-wise trained NMF controllers, however they reported a less severe degradation of performance. This may be attributed to differences in the hardware setup and implementation. Their study utilized high-density EMG grids and while relying on a subset of sensors, electrode shift was simulated by switching the channel sources to the adjacent column of electrodes. Although the electrode columns were also 1-cm apart, the change in skin-electrode impedance can be expected to be much less compared to physical shifting. Moreover, they relied on monopolar recordings while we used the bipolar montage that is typical of commercial systems. Finally, their study was conducted with a high-end benchtop bio-amplifier which sampled at a much higher frequency (2048Hz) compared to the Myo Armband (200Hz).

Although provided with training data that is enriched with combined DoF movements, the NMF-C controllers were less intuitive and performed worse than their classically trained counterparts in unperturbed scenarios. This highlights the disadvantage of naively extending the training sets to account and promote the intrinsically provided functionality. Though more diverse data sets often lead to more robust performance of the machine learning based estimators [13], this as well was not a case here. The two controllers yielded similar performance while perturbed, with NMF-C initially requiring higher efforts to be trained.

These results can be potentially explained by the fact that NMF algorithm allocates extracted basis activations to the orthogonal directions in the task space. Instead, a consideration of a more principled approach to building an intuitive synergy-inspired controller would recognize that forearm muscle synergies do not strictly operate in the reference orthogonal wrist DoFs. Such controller may then consider a rough model of forearm biomechanics where basis synergies drive movement in directions that are physiologically relatable. Similar, model-based approaches have been explored by Berger et al. [26] in force control experiments where the pulling vector of each synergy is estimated from the weighted force vectors of its constituent muscles which, themselves, are obtained via linear regression.

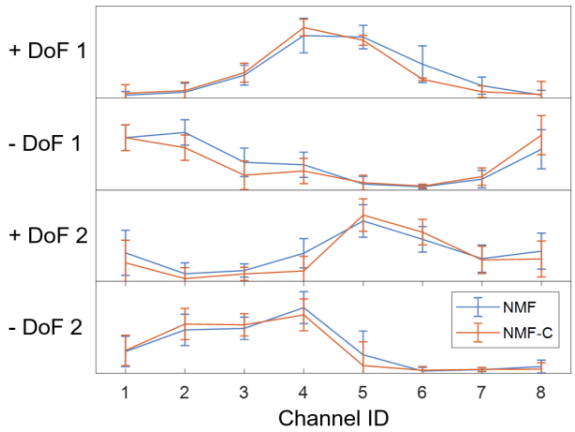

Figure 6. Averaged synergies from all subjects. The DoF-wise trained NMF results in a denser synergy matrix with more synergy overlap in sensor space. This overlap is reduced in the solutions obtained using NMF-C as the additive bases become more separable from one another.

V. Conclusions

This study compared the classic implementation of synergy-inspired myoelectric control (NMF) to its variation that considers more comprehensive training sets (NMF-C). While traditional NMF controllers were initialized from single-DoF data, here, NMF-C controllers utilized a combination of single and concurrent DoF activations during training. Online experiments revealed NMF-C to underperform due to unintuitive mappings though control was somewhat less sensitive to electrode perturbations. Conversely, NMF control yielded a high baseline performance although significant deterioration was found following the electrode shift. Despite the impaired control, the performance of NMF in electrode shifted conditions was still

on par with NMF-C. This indicated that naïve inclusion of more descriptive data during the training of these type of controllers does not yield additional benefits and further work should be done to address this trade-off between baseline performance and robustness to electrode shift. Concepts that warrant further investigation include more targeted adaptive controllers that compensate for non-stationarities and model-based approaches for interpreting synergy excitations.

REFERENCES

[1] D. Farina and O. Aszmann, "Bionic Limbs: Clinical Reality and Academic Promises," *Sci. Transl. Med.*, vol. 6, no. 257, p. 257ps12-257ps12, Oct. 2014.

[2] I. Vujaklija, D. Farina, and O. Aszmann, "New developments in prosthetic arm systems," *Orthop. Res. Rev.*, vol. Volume 8, pp. 31–39, Jul. 2016.

[3] E. Biddiss and T. Chau, "Upper-limb prosthetics: critical factors in device abandonment.," *Am. J. Phys. Med. Rehabil.*, vol. 86, no. 12, pp. 977–87, Dec. 2007.

[4] E. A. Biddiss and T. T. Chau, "Upper limb prosthesis use and abandonment: A survey of the last 25 years."

[5] B. Hudgins, P. Parker, and R. N. Scott, "A new strategy for multifunction myoelectric control," *IEEE Trans. Biomed. Eng.*, vol. 40, no. 1, pp. 82–94, Jan. 1993.

[6] K. Englehart, B. Hudgins, P. a Parker, and M. Stevenson, "Classification of the myoelectric signal using time-frequency based representations," *Med. Eng. Phys.*, vol. 21, no. 6–7, pp. 431–8, 1999.

[7] N. Jiang, H. Rehbaum, I. Vujaklija, B. Graimann, and D. Farina, "Intuitive, Online, Simultaneous, and Proportional Myoelectric Control Over Two Degrees-of-Freedom in Upper Limb Amputees," *IEEE Trans. Neural Syst. Rehabil. Eng.*, vol. 22, no. 3, pp. 501–510, May 2014.

[8] J. M. Hahne, M. A. Schweisfurth, M. Koppe, and D. Farina, "Simultaneous control of multiple functions of bionic hand prostheses: Performance and robustness in end users," *Sci. Robot.*, vol. 3, no. 19, p. eaat3630, Jun. 2018.

[9] I. Vujaklija, V. Shalchyan, E. N. Kamavuako, N. Jiang, H. R. Marateb, and D. Farina, "Online mapping of EMG signals into kinematics by autoencoding.," *J. Neuroeng. Rehabil.*, vol. 15, no. 1, p. 21, Mar. 2018.

[10] M. Sartori, J. van de Riet, and D. Farina, "Estimation of phantom arm mechanics about four degrees of freedom after targeted muscle reinnervation," *IEEE Trans. Med. Robot. Bionics*, vol. In Press, pp. 1–1, 2019.

[11] D. L. Crouch and H. Huang, "Lumped-parameter electromyogram-driven musculoskeletal hand model: A potential platform for real-time prosthesis control," *J. Biomech.*, vol. 49, no. 16, pp. 3901–3907, Dec. 2016.

[12] Ning Jiang, S. Dosen, K.-R. Muller, and D. Farina, "Myoelectric Control of Artificial Limbs—Is There a Need to Change Focus? [In the Spotlight]," *IEEE Signal Process. Mag.*, vol. 29, no. 5, pp. 152–150, Sep. 2012.

[13] L. Hargrove, K. Englehart, and B. Hudgins, "A training strategy to reduce classification degradation due to electrode displacements in pattern recognition based myoelectric control," *Biomed. Signal Process. Control*, vol. 3, no. 2, pp. 175–180, Apr. 2008.

[14] C. Prahm, B. Paassen, A. Schulz, B. Hammer, and O. Aszmann, "Transfer Learning for Rapid Re-calibration of a Myoelectric Prosthesis After Electrode Shift," 2017, pp. 153–157.

[15] J. M. Hahne, M. Markovic, and D. Farina, "User adaptation in Myoelectric Man-Machine Interfaces," *Sci. Rep.*, vol. 7, no. 1, p. 4437, Dec. 2017.

[16] S. Muceli, N. Jiang, and D. Farina, "Extracting signals robust to electrode number and shift for online simultaneous and proportional myoelectric control by factorization algorithms," *IEEE Trans. Neural Syst. Rehabil. Eng.*, vol. 22, no. 3, pp. 623–633, May 2014.

[17] J. M. Hahne, S. Dahne, H.-J. Hwang, K.-R. Muller, and L. C. Parra, "Concurrent Adaptation of Human and Machine Improves Simultaneous and Proportional Myoelectric Control," *IEEE Trans. Neural Syst. Rehabil. Eng.*, vol. 23, no. 4, pp. 618–627, Jul. 2015.

[18] E. Scheme, K. Biron, and K. Englehart, "Improving myoelectric pattern recognition positional robustness using advanced training protocols," in *2011 Annual International Conference of the IEEE Engineering in Medicine and Biology Society*, 2011, pp. 4828–4831.

[19] C. Lin, B. Wang, N. Jiang, and D. Farina, "Robust extraction of basis functions for simultaneous and proportional myoelectric control via sparse non-negative matrix factorization," *J. Neural Eng.*, vol. 15, no. 2, p. 026017, Apr. 2018.

[20] Ning Jiang, K. B. Englehart, and P. A. Parker, "Extracting Simultaneous and Proportional Neural Control Information for Multiple-DOF Prostheses From the Surface Electromyographic Signal," *IEEE Trans. Biomed. Eng.*, vol. 56, no. 4, pp. 1070–1080, Apr. 2009.

[21] D. D. Lee and H. S. Seung, "Learning the parts of objects by non-negative matrix factorization," *Nature*, vol. 401, no. 6755, pp. 788–791, Oct. 1999.

[22] Y. Qian, S. Jia, J. Zhou, and A. Robles-Kelly, "Hyperspectral Unmixing via L1/2 Sparsity-Constrained Nonnegative Matrix Factorization," *IEEE Trans. Geosci. Remote Sens.*, vol. 49, no. 11, pp. 4282–4297, Nov. 2011.

[23] N. Jiang, I. Vujaklija, H. Rehbaum, B. Graimann, and D. Farina, "Is Accurate Mapping of EMG Signals on Kinematics Needed for Precise Online Myoelectric Control?," *IEEE Trans. Neural Syst. Rehabil. Eng.*, vol. 22, no. 3, pp. 549–558, May 2014.

[24] P. M. Fitts, "The information capacity of the human motor system in controlling the amplitude of movement," *J. Exp. Psychol.*, vol. 47, no. 6, pp. 381–391, 1954.

[25] I. S. MacKenzie, "A Note on the Information-Theoretic Basis for Fitts' Law," *J. Mot. Behav.*, vol. 21, no. 3, pp. 323–330, Sep. 1989.

[26] D. J. Berger and A. d'Avella, "Effective force control by muscle synergies.," *Front. Comput. Neurosci.*, vol. 8, p. 46, 2014.